Supporting Information

Laser ablation assists cyclization reactions of hydantoic acid: A proof for the Near Attack Conformation theory?

Lucie Kolesniková, Iker León, Elena R. Alonso, Santiago Mata and Jose L. Alonso

Grupo de Espectroscopia Molecular (GEM), Unidad Asociada CSIC, Laboratorios de Espectroscopia y Bioespectroscopia, Edificio Quifima, Universidad de Valladolid, 47011 Valladolid, Spain.

Table of content

List of Tables

List of Figures

1. Experimental methods

A commercially available sample of solid HA (>98% purity, m.p. 176 ºC) was used to prepare a rod that was placed into a home-made laser ablation nozzle. During the experimental procedure, the rod was continually rotated and translated and was ablated by a pulsed picosecond Nd:YAG laser (λ = 355 nm) with a pulse energy of 19 mJ. The molecules released into the gas phase were supersonically expanded into the vacuum chamber of the spectrometer by a pulse of Ne carrier gas at a backing pressure of 9 bar. The broadband rotational spectrum of laser ablated HA has been investigated in the frequency ranges 2 – 8 and 8 – 15 GHz using CP-FTMW spectroscopy.[1] In the lower-frequency range set-up, chirped pulses of 4 μs, created by the 50 GS s^{-1} arbitrary waveform generator, were amplified by 200 W traveling wave tube (TWT) amplifier and broadcasted across the chamber of the spectrometer through a first microwave horn. At a repetition rate of 2 Hz, a total of 91000 free induction decays (4 FID emissions per gas pulse) were received by a second microwave horn, amplified and digitized using a 50 GS s^{-1} oscilloscope. In the higher-frequency range configuration, 300 W TWT amplifier and parabolic reflectors system were used instead of the 200 W TWT amplifier and microwave horns.[2] A fast Fourier transform with a Kaiser-Bessel window was used to convert the averaged time domain spectrum to obtain the frequency domain spectrum.

The sub-Doppler resolution of the laser ablation molecular beam Fourier transform microwave (LA-MB-FTMW) spectrometer,[3] operating between 2 and 8 GHz, was used to resolve the hyperfine structure due to two ^{14}N nuclei. A short microwave pulse with a duration of 0.3 μs was applied to polarize the vaporized molecules and the detected free induction decay was converted to the frequency domain by Fourier transform. All the hyperfine components appeared as Doppler doublets (see Fig. S2) due to the coaxial configuration of the supersonic

jet and the microwave radiation. The resonance frequency was therefore determined as the arithmetic means of the two Doppler components.

2. Analysis of the rotational spectrum and conformational assignment of hydantoic acid

An excess of lines with hyperfine structure arising from nuclear quadrupole coupling interactions was observed in the broadband CP-FTMW spectrum. HA could be a reasonable carrier of these lines since it possesses two ^{14}N nuclei (see N_t and N_c in Fig.1) with non-zero quadrupolar moment (I = 1) which interacts with the electric field gradient created by the rest of the molecule at the site of these nuclei. This nuclear quadrupole coupling interaction couples the nuclear spin of these nuclei and the rotation angular momentum and makes each rotational line split into numerous components.[4] However, this complex hyperfine pattern is not the only feature that makes the interpretation of the rotational spectrum of HA rather challenging. Isolated HA can be endowed with a rich conformational landscape driven by the five single-bond rotations in its backbone (see Fig. 2a in the main text). A detailed exploration of the potential energy surface was undertaken by employing fast molecular mechanics methods (MMFFs) with the ‘‘Large scales Low Mode’’ and a Monte Carlo-based search algorithms, as implemented in MacroModel (www.schrodinger.com). In a next step, geometry optimizations and frequency calculations were performed at several levels of the theory: MP2/6-311++G(d,p), B3LYP/6-311++G(d,p) with Grimme dispersion, and B2PLYPD/aug-cc-pVTZ (Gaussian16[5]). Four conformers of HA, C_5-I, C_7-I, C_7-II, and C_5-II are predicted within an energy window of 1000 cm^{-1}. Their rotational constants (A, B, C), nuclear quadrupole coupling constants (χ_{aa}, χ_{bb}, χ_{cc}) and electric dipole moment components (μ_a, μ_b, μ_c) are summarized in Tables S1 – S4. Finally, as shown in Fig. S1, NCI plots reveled the nature of intramolecular interactions that stabilize the backbones of these conformers.

Table S1. Experimental and predicted spectroscopic parameters for the C_5-I conformer of hydantoic acid.

C_5-I

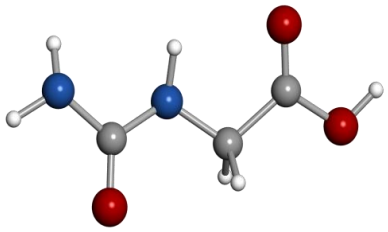

Parameter [a]	Experiment	MP2 6-311++G(d,p)	B3LYP 6-311++G(d,p) [b]	B2PLYPD aug-cc-pVTZ
A /MHz	5508.64096 (63) [c]	5408	5396	5442
B /MHz	1010.67310 (24)	1015	1016	1014
C /MHz	861.96668 (19)	868	871	867
χ_{aa} (N_c) /MHz	2.6105 (90)	2.67	2.82	2.81
χ_{bb} (N_c) /MHz	2.145 (15)	2.16	2.38	2.29
χ_{cc} (N_c) /MHz	−4.756 (15)	−4.83	−5.21	−5.11
χ_{aa} (N_t) /MHz	2.0661 (94)	2.11	2.22	2.21
χ_{bb} (N_t) /MHz	1.977 (17)	1.36	1.67	1.74
χ_{cc} (N_t) /MHz	−4.043 (17)	−3.47	−3.89	−3.95
$\lvert\mu_a\rvert$ /D	Yes [d]	1.2	1.2	1.2
$\lvert\mu_b\rvert$ /D	Yes	1.8	2.0	1.9
$\lvert\mu_c\rvert$ /D	No	0.9	1.1	0.9
N_{rot}/N_{hfs}	8 / 56	…	…	…
σ_{fit} / kHz	2.5	…	…	…
ΔE / cm^{-1}	...	0	0	0
ΔG/ cm^{-1}	...	0	0	0

[a] A, B, and C are the rotational constants; χ_{aa}, χ_{bb},and χ_{cc} are the diagonal elements of the nuclear quadrupole coupling tensor for the central (N_c) and terminal (N_t) ^{14}N nuclei; $|\mu_a|$, $|\mu_b|$ and $|\mu_c|$ are the absolute values of the electric dipole moment components along the inertial axis a, b, c; N_{rot} and N_{hfs} represent the number of fitted rotational transitions and hyperfine components, respectively; σ_{fit} is the root mean square deviation of the fit; ΔE and ΔG represent the relative energy and Gibbs free energy (T = 298 K), respectively, with respect to the global minimum. [b] Grimme dispersion taken into consideration. [c] The numbers in parentheses are 1σ uncertainties in units of the last decimal digit. [d] Experimental observation of a given type of transition.

Table S2. Experimental and predicted spectroscopic parameters for the C_7-I conformer of hydantoic acid.

C_7-I

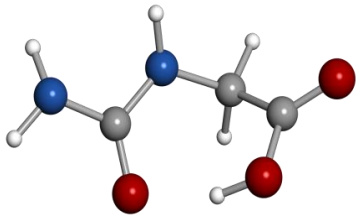

Parameter [a]	Experiment	MP2 6-311++G(d,p)	B3LYP 6-311++G(d,p) [b]	B2PLYPD aug-cc-pVTZ
A /MHz	4794.0228 (20) [c]	4642	4754	4746
B /MHz	1266.88614 (47)	1279	1265	1273
C /MHz	1103.59640 (40)	1117	1099	1109
χ_{aa} (N_c) /MHz	1.372 (11)	1.35	1.50	1.48
χ_{bb} (N_c) /MHz	0.698 (16)	0.12	0.52	0.52
χ_{cc} (N_c) /MHz	–2.070 (16)	−1.47	–2.02	–2.00
χ_{aa} (N_t) /MHz	1.7569 (86)	2.01	2.18	2.08
χ_{bb} (N_t) /MHz	1.559 (14)	1.90	2.08	1.94
χ_{cc} (N_t) /MHz	–3.316 (14)	–3.90	–4.26	–4.02
$\lvert\mu_a\rvert$ /D	Yes [d]	5.5	6.0	5.8
$\lvert\mu_b\rvert$ /D	Yes	3.6	3.8	3.7
$\lvert\mu_c\rvert$ /D	No	0.6	0.5	0.4
N_{rot}/N_{hfs}	7 / 26	…	…	…
σ_{fit} / kHz	3.3	…	…	…
ΔE / cm^{-1}	…	281	44	322
ΔG/ cm^{-1}	…	746	529	389

[a] A, B, and C are the rotational constants; χ_{aa}, χ_{bb},and χ_{cc} are the diagonal elements of the nuclear quadrupole coupling tensor for the central (N_c) and terminal (N_t) ^{14}N nuclei; $|\mu_a|$, $|\mu_b|$ and $|\mu_c|$ are the absolute values of the electric dipole moment components along the inertial axis a, b, c; N_{rot} and N_{hfs} represent the number of fitted rotational transitions and hyperfine components, respectively; σ_{fit} is the root mean square deviation of the fit; ΔE and ΔG represent the relative energy and Gibbs free energy (T = 298 K), respectively, with respect to the global minimum. [b] Grimme dispersion taken into consideration. [c] The numbers in parentheses are 1σ uncertainties in units of the last decimal digit. [d] Experimental observation of a given type of transition.

Table S3. Experimental and predicted spectroscopic parameters for the C_7-II conformer of hydantoic acid.

C_7-II

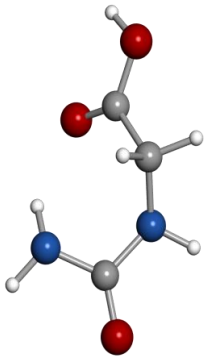

Parameter [a]	Experiment	MP2 6-311++G(d,p)	B3LYP 6-311++G(d,p) [b]	B2PLYPD aug-cc-pVTZ
A /MHz	5195.4 (12) [c]	5232	5227	5239
B /MHz	1160.2744 (19)	1156	1158	1161
C /MHz	1032.3768 (14)	1023	1015	1025
χ_{aa} (N_c) /MHz	2.057 (14)	2.09	2.22	2.20
χ_{bb} (N_c) /MHz	0.384 (48)	0.68	0.82	0.75
χ_{cc} (N_c) /MHz	–2.440 (48)	–2.77	–3.05	–2.94
χ_{aa} (N_t) /MHz	1.299 (21)	1.28	1.49	1.41
χ_{bb} (N_t) /MHz	1.562 (94)	2.00	2.21	2.08
χ_{cc} (N_t) /MHz	–2.862 (94)	–3.28	–3.69	–3.48
$\lvert\mu_a\rvert$ /D	Yes [d]	4.1	4.4	4.4
$\lvert\mu_b\rvert$ /D	No	0.3	0.4	0.4
$\lvert\mu_c\rvert$ /D	No	1.0	1.1	1.2
N_{rot}/N_{hfs}	7 / 14	…	…	…
σ_{fit} / kHz	3.7	…	…	…
ΔE / cm^{-1}	…	542	553	865
ΔG/ cm^{-1}	…	841	929	950

[a] A, B, and C are the rotational constants; χ_{aa}, χ_{bb},and χ_{cc} are the diagonal elements of the nuclear quadrupole coupling tensor for the central (N_c) and terminal (N_t) ^{14}N nuclei; $|\mu_a|$, $|\mu_b|$ and $|\mu_c|$ are the absolute values of the electric dipole moment components along the inertial axis a, b, c; N_{rot} and N_{hfs} represent the number of fitted rotational transitions and hyperfine components, respectively; σ_{fit} is the root mean square deviation of the fit; ΔE and ΔG represent the relative energy and Gibbs free energy (T = 298 K), respectively, with respect to the global minimum. [b] Grimme dispersion taken into consideration. [c] The numbers in parentheses are 1σ uncertainties in units of the last decimal digit. [d] Experimental observation of a given type of transition.

Table S4. Experimental and predicted spectroscopic parameters for the C5-II conformer of hydantoic acid.

C_5-II

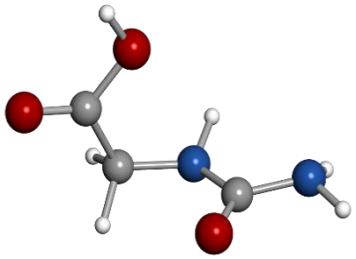

Parameter [a]	Experiment	MP2 6-311++G(d,p)	B3LYP 6-311++G(d,p) [b]	B2PLYPD aug-cc-pVTZ
A /MHz	4376.167 (22) [c]	4200	4396	4377
B /MHz	1239.283 (11)	1295	1212	1234
C /MHz	1224.5298 (81)	1286	1185	1217
χ_{aa} (N_c) /MHz	...[d]	1.22	1.47	1.41
χ_{bb} (N_c) /MHz	... [d]	2.10	0.24	–0.59
χ_{cc} (N_c) /MHz	... [d]	–3.32	–1.70	–0.82
χ_{aa} (N_t) /MHz	... [d]	1.89	1.79	1.78
χ_{bb} (N_t) /MHz	... [d]	0.12	–2.71	–3.18
χ_{cc} (N_t) /MHz	... [d]	–2.01	0.92	1.40
$\lvert\mu_a\rvert$ /D	Yes [e]	2.3	2.3	2.4
$\lvert\mu_b\rvert$ /D	Yes	3.8	3.3	2.9
$\lvert\mu_c\rvert$ /D	Yes	0.4	2.8	3.1
N_{rot}/N_{hfs}	9 / 0	…	…	…
σ_{fit} / kHz	49	…	…	…
ΔE / cm^{-1}	…	145	573	769
ΔG/ cm^{-1}	…	398	667	723

[a] A, B, and C are the rotational constants; χ_{aa}, χ_{bb},and χ_{cc} are the diagonal elements of the nuclear quadrupole coupling tensor for the central (N_c) and terminal (N_t) ^{14}N nuclei; $|\mu_a|$, $|\mu_b|$ and $|\mu_c|$ are the absolute values of the electric dipole moment components along the inertial axis a, b, c; N_{rot} and N_{hfs} represent the number of fitted rotational transitions and hyperfine components, respectively; σ_{fit} is the root mean square deviation of the fit; ΔE and ΔG represent the relative energy and Gibbs free energy (T = 298 K), respectively, with respect to the global minimum. [b] Grimme dispersion taken into consideration. [c] The numbers in parentheses are 1σ uncertainties in units of the last decimal digit. [d] Due to the weakness of individual hyperfine components, only central frequencies were analyzed. [e] Experimental observation of a given type of transition.

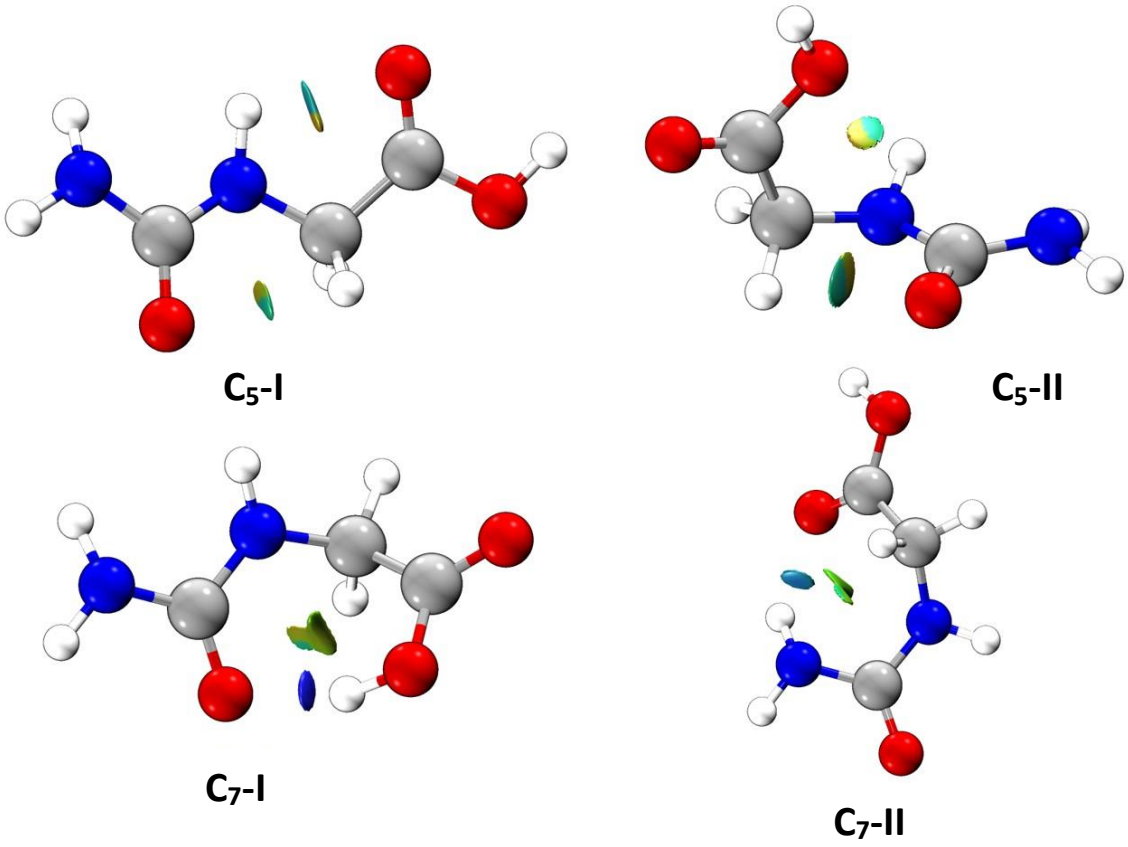

Figure S1. Non-covalent interactions (NCI) plots for the four observed conformers of hydantoic acid. Blue surfaces indicate strong attraction forces; weak interactions appear as green surfaces.

C_5-I, C_7-I, C_7-II, and C_5-II conformers were readily identified on the basis of four independent sets of *a*-type *R*-branch lines. In addition, conformers C_5-I, C_7-I, and C_5-II also presented *b*-type *R*-branch and Q-branch transitions. Finally, C_5-II conformer was the only one for which *c*-type *R*-branch and Q-branch transitions were found. These observations are in perfect agreement with predicted values of dipole moment components in Table S4. Since the spectral resolution attainable by the CP-FTMW technique was not sufficient to fully resolve the individual hyperfine components (see Fig. 1), further measurements were performed under higher resolution of our narrowband cavity-based FTMW spectrometer.[3] In this way, the hyperfine structure could be completely resolved and analyzed. The measured hyperfine components for C_5-I, C_7-I, C_7-II conformers (see Tables S5 – S7) were analyzed using the Hamiltonian $H = H_R + H_Q$, where H_R represents the rigid rotor part of the asymmetric top Hamiltonian in I^r-representation and H_Q accounts for the nuclear quadrupole coupling interactions.[4] The quadrupole coupling Hamiltonian H_Q was set up in the coupled basis set

(I_1I_2IJF), $I_1 + I_2 = I$, $I + J = F$. The energy levels involved in each transition are thus labeled with the quantum numbers J, K_a, K_c, I, F. This analysis provided accurate values of the rotational constants and the diagonal elements of the nuclear quadrupole coupling tensor given in Table 1 and Tables S1 – S3. Unfortunately, the weakness of the spectral features of C_5-II conformer and, consequently, the small number of experimentally available hyperfine components prevented their unambiguous assignment and the frequency centers (see Table S8) were thus fitted to determine the rotational constants from Tables 1 and S4.

Table S5. Fitted rotational transitions of the C_5-I conformer of hydantoic acid.

J'	K_a'	K_c'	I'	F'	J''	K_a''	K_c''	I''	F''	Obs. Freq. (MHz)	Obc.-Cal. (MHz)	Uncertainty (MHz)
1	1	1	2	1	0	0	0	2	2	6369.255	0.000	0.005
1	1	1	1	1	0	0	0	1	1	6370.090	-0.003	0.005
1	1	1	2	3	0	0	0	2	2	6370.403	0.001	0.005
1	1	1	1	2	0	0	0	1	1	6370.710	0.000	0.005
1	1	1	0	1	0	0	0	0	0	6371.236	0.000	0.005
1	1	1	1	0	0	0	0	1	1	6371.639	0.001	0.005
2	0	2	2	4	1	0	1	2	3	3741.542	0.004	0.005
2	0	2	1	2	1	0	1	1	1	3741.628	0.002	0.005
2	0	2	1	3	1	0	1	1	2	3741.708	0.003	0.005
2	0	2	2	2	1	0	1	2	2	3741.891	-0.001	0.005
2	0	2	2	2	1	0	1	0	1	3742.000	0.002	0.005
2	0	2	0	2	1	0	1	2	1	3742.391	0.003	0.005
2	0	2	2	1	1	0	1	2	1	3742.579	-0.002	0.005
2	0	2	1	1	1	0	1	1	1	3742.849	0.001	0.005
3	0	3	2	5	2	0	2	2	4	5603.345	0.002	0.005
3	0	3	2	4	2	0	2	2	3	5603.388	0.003	0.005
3	0	3	1	4	2	0	2	1	3	5603.464	0.000	0.005
3	0	3	0	3	2	0	2	0	2	5603.491	0.001	0.005
3	0	3	2	3	2	0	2	2	2	5603.580	0.001	0.005
3	0	3	2	2	2	0	2	2	1	5603.772	0.001	0.005
3	0	3	2	3	2	0	2	2	3	5603.933	-0.001	0.005
4	0	4	2	6	3	0	3	2	5	7454.341	-0.005	0.005
4	0	4	2	4	3	0	3	2	3	7454.548	-0.007	0.005
4	0	4	2	3	3	0	3	2	2	7454.570	-0.006	0.005
4	0	4	1	5	3	0	3	1	4	7454.450	-0.005	0.005
4	0	4	1	4	3	0	3	1	3	7454.365	-0.006	0.005
3	1	2	1	4	2	1	1	1	3	5838.710	0.001	0.005
3	1	2	2	5	2	1	1	2	4	5838.633	0.002	0.005
3	1	2	2	4	2	1	1	2	3	5838.916	0.003	0.005
3	1	2	2	3	2	1	1	2	2	5838.906	0.000	0.005

3	1	2	1	3	2	1	1	1	2	5838.534	0.003	0.005
3	1	2	0	3	2	1	1	0	2	5838.420	0.003	0.005
3	1	3	2	5	2	1	2	2	4	5392.416	0.003	0.005
3	1	3	1	3	2	1	2	1	2	5392.470	0.001	0.005
3	1	3	1	2	2	1	2	1	1	5392.535	0.001	0.005
3	1	3	2	4	2	1	2	2	3	5392.625	-0.002	0.005
3	1	3	0	3	2	1	2	0	2	5392.637	0.003	0.005
3	1	3	1	4	2	1	2	1	3	5392.717	0.003	0.005
3	1	3	2	3	2	1	2	2	2	5393.055	0.002	0.005
3	1	3	2	2	2	1	2	2	1	5393.208	0.001	0.005
1	1	0	1	0	1	0	1	1	1	4645.049	0.001	0.005
1	1	0	2	2	1	0	1	2	3	4645.363	0.001	0.005
1	1	0	0	1	1	0	1	2	1	4646.874	-0.002	0.005
1	1	0	1	2	1	0	1	1	1	4647.033	-0.001	0.005
1	1	0	1	1	1	0	1	1	2	4647.651	-0.003	0.005
1	1	0	2	1	1	0	1	2	2	4648.746	-0.002	0.005
1	1	0	2	1	1	0	1	0	1	4648.854	0.001	0.005
2	1	2	2	4	1	0	1	2	3	8094.146	-0.001	0.005
2	1	2	1	2	1	0	1	1	1	8094.025	0.001	0.005
2	1	2	1	1	1	0	1	1	0	8094.481	-0.002	0.005
2	1	2	0	2	1	0	1	2	1	8094.636	0.001	0.005
2	1	2	1	3	1	0	1	1	2	8094.735	0.002	0.005
2	1	2	2	2	1	0	1	0	1	8095.738	0.000	0.005
2	1	2	2	3	1	0	1	2	3	8096.047	0.003	0.005
2	1	2	1	1	1	0	1	1	1	8096.227	0.002	0.005
2	1	2	1	2	1	0	1	1	2	8093.342	0.000	0.005

Table S5. Fitted rotational transitions of the C_7-I conformer of hydantoic acid.

J'	K_a'	K_c'	*I'*	*F'*	*J''*	K_a''	K_c''	*I''*	*F''*	Obs. Freq. (MHz)	Obc.-Cal. (MHz)	Uncertainty (MHz)
2	1	2	2	4	1	1	1	2	3	4577.409	0.005	0.005
2	1	2	1	2	1	1	1	1	1	4577.280	0.002	0.005
2	1	2	2	3	1	1	1	2	2	4578.077	0.004	0.005
2	1	2	2	2	1	1	1	0	1	4578.483	0.001	0.005
2	0	2	2	4	1	0	1	2	3	4735.346	-0.001	0.005
2	0	2	1	3	1	0	1	1	2	4735.461	0.002	0.005
2	0	2	2	2	1	0	1	0	1	4735.664	0.000	0.005
2	0	2	0	2	1	0	1	2	1	4735.910	-0.002	0.005
2	0	2	1	2	1	0	1	2	1	4736.061	0.000	0.005
2	0	2	1	1	1	0	1	1	1	4736.230	-0.001	0.005
2	1	1	2	2	1	1	0	0	1	4904.608	0.006	0.005
2	1	1	2	3	1	1	0	2	2	4904.846	-0.004	0.005

1	1	1	2	1	0	0	0	2	2	5896.797	-0.001	0.005
1	1	1	1	1	0	0	0	1	1	5897.384	-0.003	0.005
1	1	1	2	3	0	0	0	2	2	5897.511	0.005	0.005
1	1	1	1	2	0	0	0	1	1	5897.643	0.001	0.005
3	1	3	2	5	2	1	2	2	4	6862.973	-0.002	0.005
3	1	3	1	3	2	1	2	1	2	6862.991	-0.009	0.005
3	1	3	1	4	2	1	2	1	3	6863.153	0.002	0.005
3	1	3	2	3	2	1	2	2	2	6863.382	-0.005	0.005
3	1	3	2	2	2	1	2	2	1	6863.445	0.004	0.005
3	1	2	2	5	2	1	1	2	4	7352.816	0.000	0.005
3	1	2	1	4	2	1	1	1	3	7352.903	0.003	0.005
3	1	2	1	3	2	1	1	1	2	7352.761	-0.003	0.005
3	1	2	2	2	2	1	1	2	1	7352.676	-0.001	0.005
1	1	0	2	3	1	0	1	2	3	3690.850	-0.002	0.005

Table S7. Fitted rotational transitions of the C_7-II conformer of hydantoic acid.

J'	K_a'	K_c'	*I'*	*F'*	*J''*	K_a''	K_c''	*I''*	*F''*	Obs. Freq. (MHz)	Obc.-Cal. (MHz)	Uncertainty (MHz)
3	0	3	2	5	2	0	2	2	4	6565.939	-0.001	0.005
3	0	3	2	4	2	0	2	2	3	6565.961	0.001	0.005
3	0	3	1	4	2	0	2	1	3	6566.015	-0.001	0.005
3	0	3	2	3	2	0	2	2	2	6566.091	0.002	0.005
2	0	2	1	3	1	0	1	1	2	4382.336	-0.002	0.005
2	0	2	2	4	1	0	1	2	3	4382.229	-0.002	0.005
2	1	1	1	3	1	1	0	1	2	4513.363	0.001	0.010
2	1	1	2	4	1	1	0	2	3	4513.077	0.003	0.010
3	1	3	2	3	2	1	2	2	2	6384.547	-0.002	0.010
3	0	3	2	2	2	0	2	2	1	6566.236	-0.002	0.010
1	0	1	2	1	0	0	0	2	2	2191.505	0.000	0.010
1	0	1	2	3	0	0	0	2	2	2192.476	-0.007	0.010
1	0	1	1	2	0	0	0	1	1	2192.725	0.008	0.010
2	1	2	2	4	1	1	1	2	3	4257.130	0.007	0.010

Table S8. Fitted rotational transitions (central frequencies) of the C_5-II conformer of hydantoic acid.

J'	K_a'	K_c'	J''	K_a''	K_c''	Obs. Freq. (MHz)	Obc.-Cal. (MHz)	Uncertainty (MHz)
2	0	2	1	0	1	4927.609	0.044	0.050
2	1	1	1	1	0	4942.308	-0.072	0.050
2	1	2	1	1	1	4912.790	-0.065	0.050
1	1	1	0	0	0	5600.680	0.004	0.050
1	1	0	1	0	1	3151.639	0.009	0.050
3	0	3	2	1	1	4224.755	-0.019	0.050
3	0	3	2	1	2	4269.114	0.054	0.050
1	1	0	0	0	0	5615.403	-0.036	0.050
2	1	2	1	0	1	8049.780	0.057	0.050

Table S9. Experimental and predicted spectroscopic parameters for 2,5-oxazolidinedione.

Parameter [a]	Experimental	MP2 6-311++G(d,p)	B3LYP 6-311++G(d,p) [b]	B2PLYPD aug-cc-pVTZ
A /MHz	6550.6445 (14) [c]	6551	6561	6587
B /MHz	2391.76565 (60)	2375	2378	2382
C /MHz	1772.88748 (54)	1763	1765	1769
P_c /uÅ^2	1.694614 (52)	1.64	1.61	1.60
χ_{aa} /MHz	2.5587 (80)	2.68	2.78	2.62
χ_{bb} /MHz	2.2353 (69)	2.44	2.56	2.35
χ_{cc} /MHz	–4.7940 (69)	–5.12	–5.34	–4.97
$\lvert\mu_a\rvert$ /D	No [d]	0.4	0.3	0.3
$\lvert\mu_b\rvert$ /D	Yes	5.1	5.3	5.1
$\lvert\mu_c\rvert$ /D	No	0.0	0.0	0.0
N_{rot}/ N_{hfs}	6 / 21	…	…	…
σ_{fit} / MHz	0.005	…	…	…

[a] A, B, and C are the rotational constants; P_c is the planar moment of inertia; χ_{aa}, χ_{bb},and χ_{cc} are the diagonal elements of the nuclear quadrupole coupling tensor for the ^{14}N nuclei; $|\mu_a|$, $|\mu_b|$ and $|\mu_c|$ are the absolute values of the electric dipole moment components along the inertial axis a, b, c; N_{rot} and N_{hfs} represent the number of fitted rotational transitions and hyperfine components, respectively; σ_{fit} is the root mean square deviation of the fit. [b] Grimme dispersion taken into consideration. [c] The numbers in parentheses are 1σ uncertainties in units of the last decimal digit. [d] Experimental observation of a-, b-, and c-type transitions.

Table S10. Fitted rotational transitions of 2,5-oxazolidinedione.

J'	K_a'	K_c'	F'	J''	K_a''	K_c''	F''	Obs. Freq. (MHz)	Obs.-Cal. (MHz)	Uncertainty (MHz)
2	0	2	3	1	1	1	2	4106.259	-0.006	0.010
1	1	0	1	1	0	1	1	4775.915	-0.004	0.010
1	1	0	1	1	0	1	2	4776.678	-0.008	0.010
1	1	0	2	1	0	1	1	4777.356	-0.001	0.010
1	1	0	2	1	0	1	2	4778.119	-0.006	0.010
1	1	0	0	1	0	1	1	4779.511	-0.004	0.010
2	1	1	2	2	0	2	2	5459.381	0.002	0.010
2	1	1	3	2	0	2	2	5460.102	0.005	0.010
2	1	1	3	2	0	2	3	5461.072	0.003	0.010
2	1	1	1	2	0	2	1	5462.003	-0.006	0.010
3	1	2	3	3	0	3	3	6597.201	0.002	0.010
3	1	2	4	3	0	3	4	6598.913	0.005	0.010
3	1	2	2	3	0	3	2	6599.503	-0.004	0.010
1	1	1	1	0	0	0	1	8324.096	0.006	0.010
1	1	1	2	0	0	0	1	8323.421	0.001	0.010
3	0	3	3	2	1	2	2	8637.823	-0.004	0.010
3	0	3	4	2	1	2	3	8638.130	-0.008	0.010
3	0	3	2	2	1	2	1	8638.574	0.011	0.010
2	1	2	3	1	0	1	2	11869.092	-0.001	0.010
2	1	2	1	1	0	1	0	11869.392	0.004	0.010
2	1	2	2	1	0	1	1	11869.865	-0.001	0.010

3. Spectral identification and analysis of 2,5-oxazolidinedione

The structure of 2,5-oxazolidinedione has been calculated at three different levels of theory: MP2/6-311++G(d,p), B3LYP/6-311++G(d,p) with Grimme dispersion, and B2PLYPD/aug-cc-pVTZ (see Table S9) and the predicted spectral features were contrasted with the broadband CP-FTMW spectrum. Three *b*-type *Q*-branch transitions and one *b*-type *R*-branch transition could be identified. Ignoring the hyperfine effects and following an iterative procedure of fitting and predictions, more *b*-type *R*-branch transitions were successfully assigned after the extension of the experimental spectrum up to 15 GHz. Neither *a*- nor *c*-type transitions were observed in accordance with the nearly zero values of the predicted dipole moment components (see Table S9). Another hallmark of the spectrum was the observation of

only three $\Delta F = 1$ hyperfine components for $1_{1\,1} \leftarrow 0_{0\,0}$ transition which corroborates the nuclear quadrupole interactions of single ^{14}N nuclei. The list of measured hyperfine frequencies is given in Table S10. They were analyzed using the Hamiltonian $H = H_R + H_Q$, where H_R corresponds to the rigid rotor Hamiltonian in I^r-representation and H_Q accounts for the nuclear quadrupole coupling interactions. In this case, the $F = J + I$ angular momentum coupling scheme was applied to label the hyperfine sub-levels by J, K_a, K_c, and F quantum numbers. This analysis provided the spectroscopic parameters shown in Tables 2 and S9. Their values allow a first structural assessment of 2,5-oxazolidinedione. Planar moment of inertia $P_c = ½(I_a + I_b - I_c)$, gives information about the mass extension out of the *ab* inertial plane and points towards a nearly planar heavy atom skeleton with one pair of out-of-plane hydrogens, like in hydantoin (see Fig. S2).[6] In view of this structure, the χ_{cc} component of the nuclear quadrupole coupling tensor is expected to be unchanged during the transformation from the principal inertial axes to principal quadrupolar axis. Hence, its value can be taken as a reporter on the electric field gradient along the direction of an axis perpendicular to the heterocyclic ring. The experimental value χ_{cc} confirms the presence in 2,5-oxazolidinone of pyrrole-like nitrogen that experiences very similar chemical environment as the amide nitrogen in hydantoin (see Fig. S2).

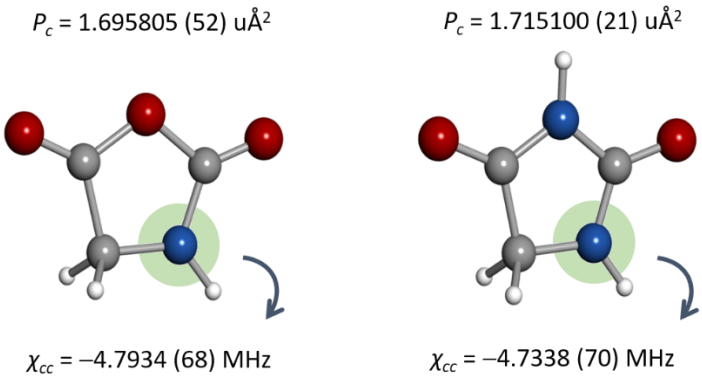

Figure S2. Comparison of the values of planar moment of inertia and χ_{cc} component of the nuclear quadrupole coupling tensor for 2,5-oxazolidinedione with those for hydantoin.

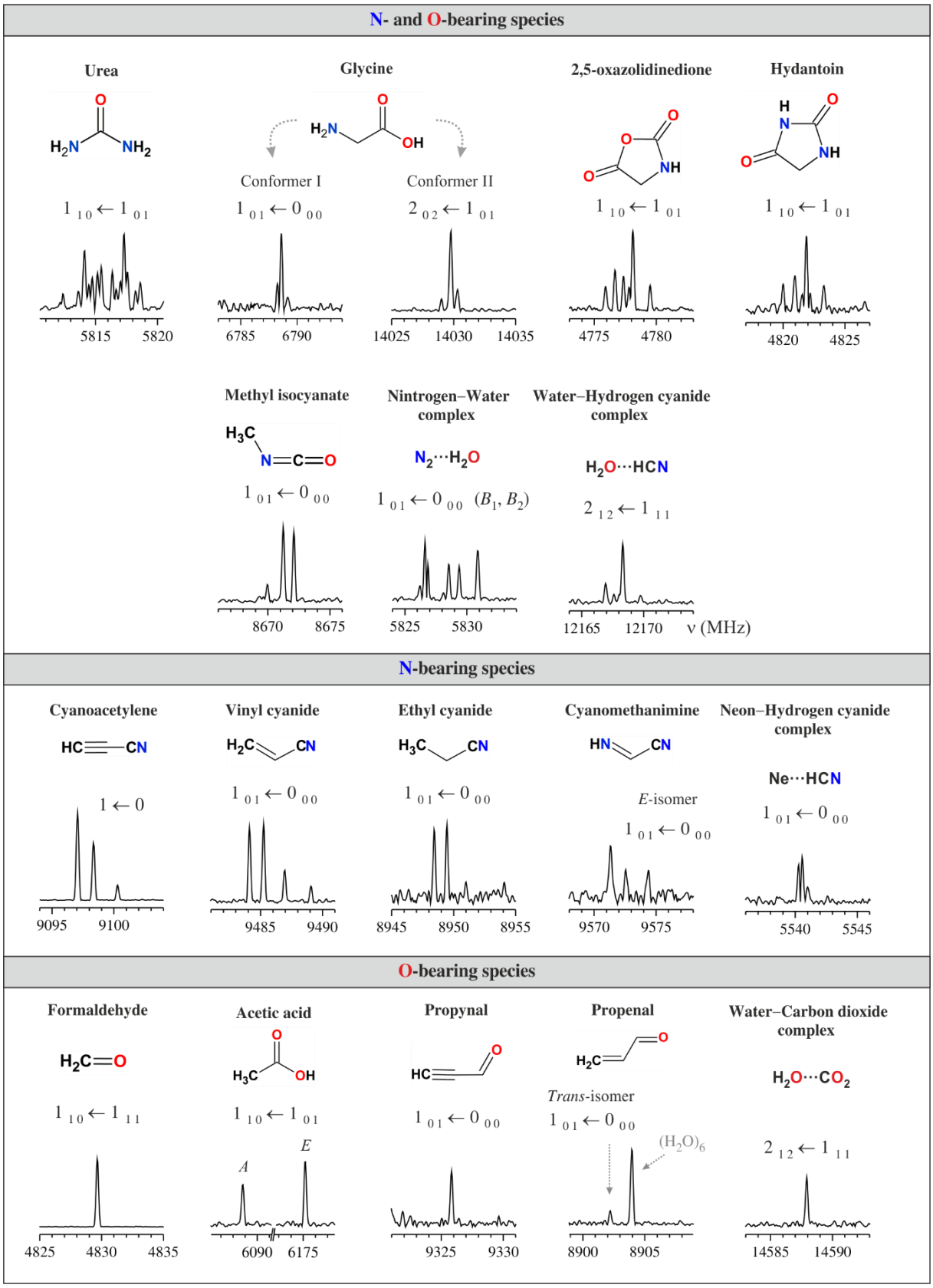

Figure S3. Selected rotational transitions of detected species other than hydantoic acid.

4. Identification of different molecular species

Eleven additional monomer species and four molecular complexes were identified by detailed inspection of published frequencies in spectroscopic/astrophysical databases (Madex,[7] CDMS,[8] JPL,[9] and Splatalogue[10]) and microwave literature. A selection of rotational transitions of these species is shown in Fig. S3. Of all these molecules, glycine has been observed through its two most stable conformers, but only the *trans* and *E* isomers of propenal and cyanomethanimine, respectively, were detected.

References

(1) Brown, G. G.; Dian, B. C.; Douglass, K. O.; Geyer, S. M.; Shipman, S. T.; Pate, B. H. A Broadband Fourier Transform Microwave Spectrometer Based on Chirped Pulse Excitation. *Rev. Sci. Instrum.* **2008**, *79* (5), 53103.

(2) Pena, I.; Mata, S.; Martin, A.; Cabezas, C.; Daly, A. M.; Alonso, J. L. Conformations of D-Xylose: The Pivotal Role of the Intramolecular Hydrogen-Bonding. *Phys. Chem. Chem. Phys.* **2013**, *15* (41), 18243–18248.

(3) Bermúdez, C.; Mata, S.; Cabezas, C.; Alonso, J. L. Tautomerism in Neutral Histidine. *Angew. Chemie Int. Ed.* **2014**, *53* (41), 11015–11018.

(4) Gordy, W.; Cook, R. L. *Microwave Molecular Spectra*; Wiley: New York, 1984.

(5) M. J. Frisch, G. W. Trucks, H. B. Schlegel, G. E. Scuseria, M. A. Robb, J. R. Cheeseman, G. Scalmani, V. Barone, G. A. Petersson, H. Nakatsuji, X. Li, M. Caricato, A. V. Marenich, J. Bloino, B. G. Janesko, R. Gomperts, B. Mennucci, H. P. Hratchian, J. V., 2016. Gaussian 16, Revision A.03. Gaussian, Inc.: Wallingford, CT.

(6) Alonso, E. R.; Kolesniková, L.; Alonso, J. L. Laser Ablated Hydantoin: A High Resolution Rotational Study. *J. Chem. Phys.* **2017**, *147* (12), 124312.

(7) Cernicharo, J. Laboratory Astrophysics and Astrochemistry in the Herschel/ALMA Era. *Proc. Eur. Conf. Lab. Astrophys. EAS Publ. Ser.* **2012**, *58*, 251–261.

(8) Müller, H. S. P.; Thorwirth, S.; Roth, D. A.; Winnewisser, G. The Cologne Database for Molecular Spectroscopy, CDMS. *Astron. Astrophys.* **2001**, *370* (3), L49–L52. Available at: https://www.astro.uni-koeln.de/cdms/molecules (as of 11/2018).

(9) Pickett, H. M.; Poynter, R. L.; Cohen, E. A.; Delitsky, M. L.; Pearson, J. C.; MÜLler, H. S. P. SUBMILLIMETER, MILLIMETER, AND MICROWAVE SPECTRAL LINE CATALOG. *J. Quant. Spectrosc. Rad. Transf.* **1998**, *60* (5), 883–890. JPL catalog available at: https://spec.jpl.nasa.gov/

(10) Splatalogue: database for astronomical spectroscopy https://www.cv.nrao.edu/php/splat/.